Journal of Medicinal Chemistry

pubs.acs.org/jmc

Article

MPLA-Adjuvanted Liposomes Encapsulating S-Trimer or RBD or S1, but Not S-ECD, Elicit Robust Neutralization Against SARS-CoV-2 and Variants of Concern

Jian Wang,[‖] Xu-Guang Yin,[‖] Yu Wen,[‖] Jie Lu, Ru-Yan Zhang, Shi-Hao Zhou, Chun-Miao Liao, Hua-Wei Wei, and Jun Guo*

Cite This: https://doi.org/10.1021/acs.jmedchem.1c02025

Read Online

ACCESS | Metrics & More | Article Recommendations | Supporting Information

ABSTRACT: Safe and effective vaccines are the best method to defeat worldwide SARS-CoV-2 and its circulating variants. The SARS-CoV-2 S protein and its subunits are the most attractive targets for the development of protein-based vaccines. In this study, we evaluated three lipophilic adjuvants, monophosphoryl lipid A (MPLA), Toll-like receptor (TLR) 1/2 ligand Pam_3CSK_4, and α-galactosylceramide (α-GalCer), in liposomal and nonliposomal vaccines. The immunological results showed that the MPLA-adjuvanted liposomal vaccine induced the strongest humoral and cellular immunity. Therefore, we further performed a systematic comparison of S-trimer, S-ECD, S1, and RBD as antigens in MPLA-adjuvanted liposomes and found that, although these four vaccines all induced robust specific antibody responses, only S-trimer, S1, and RBD liposomes, but not S-ECD, elicited potent neutralizing antibody responses. Moreover, RBD, S-trimer, and S1 liposomes effectively neutralized variants (B.1.1.7/alpha, B.1.351/beta, P.1/gamma, B.1.617.2/delta, and B.1.1.529/omicron). These results provide important information for the subunit vaccine design against SARS-CoV-2 and its variants.

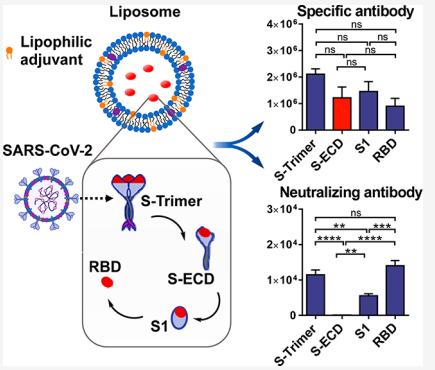

INTRODUCTION

The coronavirus disease (COVID-19) pandemic, caused by severe acute respiratory syndrome coronavirus 2 (SARS-CoV-2), has posed serious threats to public health and the global economy. Therefore, it is imperative to develop safe and effective vaccines against SARS-CoV-2 and, more importantly, the emerging variants circulating worldwide. Similar to other coronaviruses, including SARS-CoV (reported in 2002) and Middle East respiratory syndrome coronavirus (MERS-CoV, identified in 2012), spike (S) proteins on the surface of SARS-CoV-2 mainly consist of S1 and S2 domains, which are responsible for virus-cell attachment and membrane fusion, respectively (Figure 1A,B).[1] Located in the middle region of S1, the receptor binding domain (RBD) is the key component that directly binds to the host cell receptor angiotensin-converting enzyme 2 (ACE2).[1−3] Notably, in natural virions, the S protein is a trimeric class I fusion protein that exists in a prefusion conformation, which undergoes substantial structural rearrangement toward the postfusion state for eventual virus-cell membrane fusion (Figure 1C). Thus, a stabilized prefusion form of the S protein (S-trimer) was achieved by adding two stabilizing proline mutations in the C-terminal S2 fusion in previous research.[4,5] Given their indispensable functions in viral infection, the S-trimer,[6,7] S-ECD (extracellular domain),[8] S1,[9,10] and RBD[11,12] are ideal targets for developing subunit vaccines against SARS-CoV-2 and its variants. In addition, we also investigated potent COVID-19 subunit vaccines using RBD as the protein antigen.[13,14] However, few studies have systematically compared these S subunits as vaccine antigens in immunological evaluation.

In contrast to the nucleic-acid-based vaccines (DNA and mRNA), which brought the advantage of speed in the earliest days of the COVID-19 crisis, protein-based vaccines can be manufactured at relatively low cost and easily stored for widespread use, and they can be used in various populations for a better safety profile.[15] However, the weak immunogenicity of protein antigens is the most significant barrier for subunit vaccines to clinical translation; thus, subunit vaccines often require the use of immunostimulants (adjuvants), especially innate immune receptor ligands, to improve efficacy. Toll-like receptor (TLR) agonists, such as lipophilic adjuvants monophosphoryl lipid A (MPLA) and Pam_3CSK_4, have attracted considerable interest as adjuvants, as they can elicit both innate and adaptive immunity. The lipid A derivative, MPLA, is a

Received: November 25, 2021

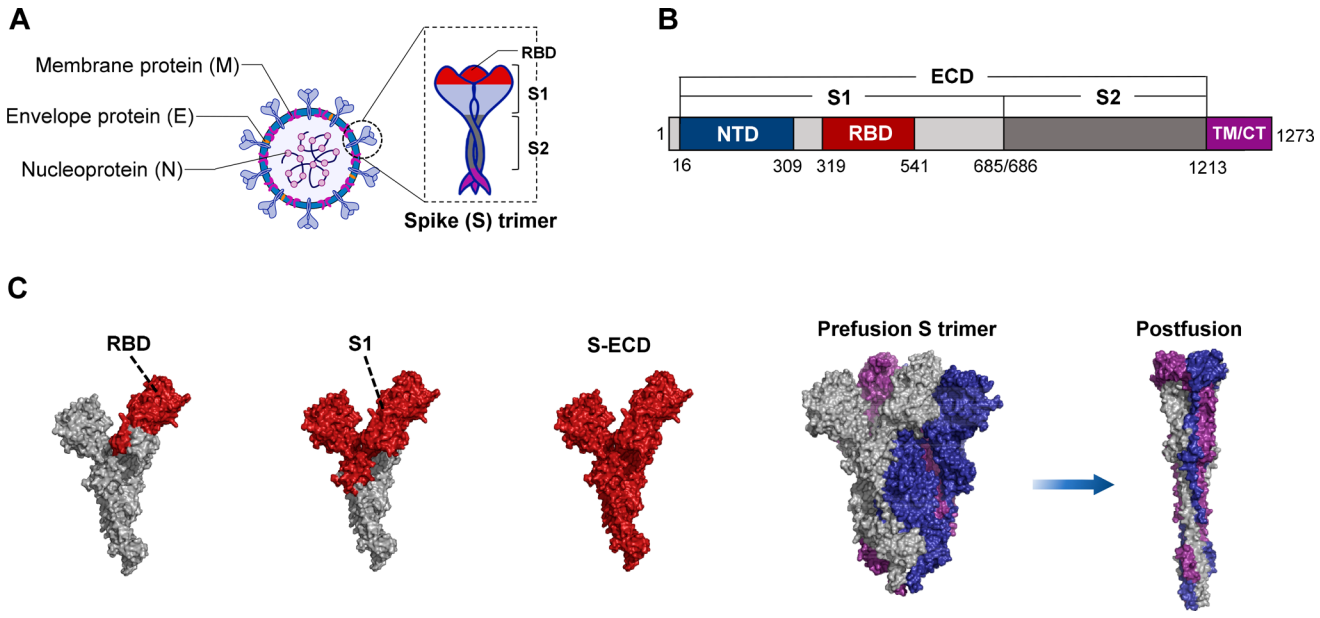

Figure 1. Key SARS-CoV-2-S target protein subunits and structural changes of S-trimer. (A) Four structural proteins of SARS-CoV-2 and major features of the S protein. (B) Linear representation of the sequence/structure elements of the full-length SARS-CoV-2 S protein. N-terminal domain (NTD, aa 16−309); receptor binding domain (RBD, aa 319−541); S1 domain of S protein (S1, aa 16−685); S2 domain of S protein (S2, aa 686−1213); transmembrane domain (TM, aa 1214−1236); cytoplasmic tail (CT, aa 1237−1273); extracellular domain of S (ECD, aa 16−1213). (C) Surface representation of S trimer in the prefusion (PDB ID: 6VXX) and postfusion (PDB ID: 6XRA) conformations. Each protomer is shown in a different color. The locations of RBD, S1, and S-ECD on the protomer are shown in red.

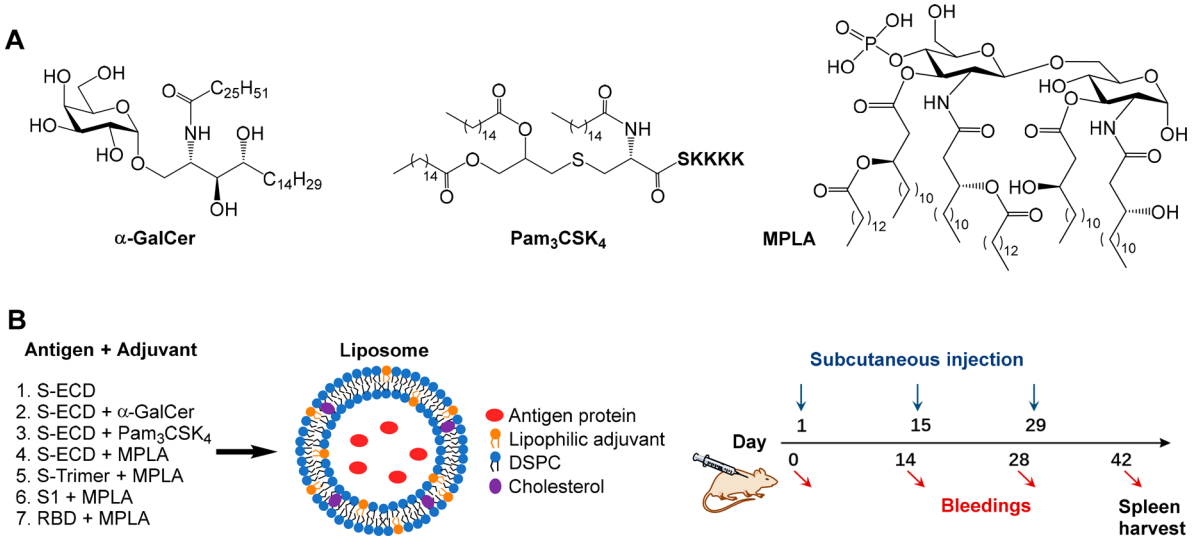

Figure 2. Molecular structures of adjuvants and formulations of liposomal vaccine candidates. (A) Molecular structures of adjuvants α-GalCer, Pam_3CSK_4 and MPLA. (B) Formulations of liposomal vaccines and vaccination schedule.

strong immunostimulant, which can interact with TLR4 to promote antigen presentation and T cell activation.[16] In contrast to lipid A, MPLA is less toxic and pyrogenic; as a result, MPLA has been used in clinically approved adjuvants AS01B and AS04.[17,18] The bacterial lipopeptide Pam_3CSK_4 is the most studied TLR1/2 agonist and has been shown to be a potent B lymphocyte and macrophage activator.[19,20] In contrast to TLR ligands, α-galactosylceramide (α-GalCer), which is present on CD1d, potently activates iNKT cells and rapidly induces the secretion of copious amounts of cytokines, including IL-4 and IFN-γ.[21,22] Besides, adjuvant aluminum gel (Alum) is the most well-accepted adjuvant for human vaccines and has a complex mechanism.[23] Alum should continue to represent the "gold standard" given its long-term success, with which all new adjuvants should be compared. Adjuvants are generally coadministrated with antigens, but this might lead to a limited enhancement of immune responses. In addition, lipophilic adjuvants, such as MPLA, Pam_3CSK_4, and α-GalCer, tend to aggregate as liposomes with their hydrophilic head groups and hydrophobic acyl chains in aqueous environments (Figure 2A). To maximize their ability to promote effective activation of immune processes, a safe and facile formulation of adjuvants and antigens is necessary to induce sufficient immune efficiency.

Due to their ability to encapsulate hydrophilic and lipophilic compounds into the inner water phase and within lipid bilayers, liposomes are ideal delivery vehicles for antigen proteins and

https://doi.org/10.1021/acs.jmedchem.1c02025
J. Med. Chem. XXXX, XXX, XXX−XXX

lipid adjuvants (Figure 2B). With high biocompatibility, biodegradability, and low toxicity, liposomes can promote the persistence, stability, and conformational integrity of antigen proteins and facilitate the gradual release of vaccine components through depot effects.[24−26] Studies have demonstrated that coformulating antigens and adjuvants in liposomes can enhance humoral and cellular immune responses compared to the mixture of compounds in nonliposomal formulations after immunization.[27−30] Moreover, codelivery of antigens and adjuvants, especially TLR ligands, such as lipophilic MPLA and Pam_3CSK_4, leads to concurrent antigen processing and presentation and TLR pathway signaling, which triggers activated dendritic cells to prime antigen-specific humoral and cellular immunity.[16,31] In addition, the lipophilic iNKT ligand α-GalCer codelivered with tumor-associated antigens[32,33] and RBD protein[13] in liposomes demonstrated satisfactory immune responses in our previous study. Collectively, developing an effective and applicable vaccine formulation with optimized antigens and adjuvants is highly attractive given the worldwide emergence caused by the rapid spread of SARS-CoV-2 variants.

Therefore, to evaluate the adjuvant effect of α-GalCer, Pam_3CSK_4, and MPLA on SARS-CoV-2 vaccines, we chose the S-ECD (S1 + S2 extracellular domain) protein as a model antigen and used the S-ECD protein plus Alum adjuvant as a control group. To explore whether liposomal formulation is superior to the physical mixture of vaccine components in terms of immune efficacy, antigen proteins add-mixed with different lipophilic adjuvants were prepared as liposomes parallel to free protein and adjuvant aggregated particles (nonliposomal formulation). Furthermore, we assessed the vaccine candidates based on S-trimer, S-ECD, S1, or RBD in both humoral and cellular responses. Meanwhile, the neutralizing activity of vaccinated mouse sera against wild-type (WT) SARS-CoV-2 pseudovirus and variants (B.1.1.7/alpha, B.1.351/beta, P.1/gamma, B.1.617.2/delta, and B.1.1.529/omicron) was evaluated. Our results will shed light on the optimization of vaccine formulation, adjuvants, and antigens and eventually provide useful information for the development of protein-based vaccines against SARS-CoV-2.

RESULTS

Vaccine Preparation and Vaccination Schedule. The liposomal vaccines were prepared using a thin-film hydration approach composed of a mixture of 1,2-distearoyl-*sn*-glycero-3-phosphocholine (DSPC), cholesterol, adjuvants, and antigen proteins. The compounds in the liposomal vaccines were mixed in PBS and sonicated with antigen proteins for the final vaccination. The molar ratio of DSPC:cholesterol:adjuvant was 8:4:1 for MPLA (8.8 μg per mouse)- and Pam_3CSK_4 (7.5 μg per mouse)-adjuvanted liposomes, and the molar ratio of α-GalCer (2 μg per mouse)-adjuvanted liposomes was 8:4:0.47 (DSPC:cholesterol:adjuvant), as a higher dose of α-GalCer injection might lead to significant iNKT anergy.[34] The amount of antigen used in the liposomal and nonliposomal groups was set as 10 μg per mouse, and the nonliposomal vaccines were prepared by physically mixing protein antigens and adjuvants in amounts equal to that of their liposomal counterparts. Dynamic light scattering (DLS) measurements showed that the average size by intensity of all liposomes was approximately 200−400 nm (Figure S1A,B). Thus, these liposome particles larger than 100 nm would rely on being phagocytosed by tissue-resident antigen-presenting cells (APCs) for transport to lymph nodes.[35] The ζ potentials of MPLA-adjuvanted liposomes were much lower than those of other controls, as MPLA is negatively charged with a phosphate group (Figure S1C,D). Liposomes provide vaccines with a relatively homogeneous size distribution and facilitate antigen and adjuvant uptake by APCs through codelivery and multivalent presentation. To immunologically evaluate different vaccine formulations, adjuvants, and antigen proteins, 13 groups of female BALB/c mice (n = 5/group, 6−8 weeks old) were immunized subcutaneously on days 0, 14, and 28. To optimize the formulation and adjuvant, the S-ECD protein was employed as a model antigen, and four groups of mice were vaccinated with liposomal formulations, while the other four groups were administered the same components in solution. In addition, a group coadministered with Alum adjuvant was used as a positive control. For antigen optimization, four additional groups were immunized with liposomes containing S-trimer, S-ECD, S1, and RBD. Mouse sera were collected on day 0 before initial immunization (negative controls) and days 14, 28, and 42 after immunization, and splenocytes were isolated from vaccinated and PBS-treated mice on day 42 (Figure 2B).

Specific Antibody Responses Induced by Vaccines Using Different Adjuvants. To investigate the impact of different adjuvants and delivery platforms on immune responses, the S-ECD-specific antibody titers of each immunization were determined by ELISA. After the last immunization, as shown in Figure 3A, the S-ECD protein added with adjuvants (α-GalCer, Pam_3CSK_4, MPLA or Alum) showed increased IgG antibodies compared to S-ECD alone in both the liposomal and nonliposomal formulations. Meanwhile, liposomal vaccines induced a higher level of IgG antibodies (Figure 3A) but lower levels of IgM antibodies (Figure S2C) than the nonliposomal formulations. These findings indicate that the liposomes could elicit a strong humoral immune response, with high efficacy in inducing antibody class switching from IgM to IgG. Among the liposomal vaccines, S-ECD/MPLA induced the highest antibody titers, with ∼10- and ∼2-fold increases compared to the S-ECD and S-ECD/Al controls, respectively, whereas S-ECD/α-GalCer and S-ECD/Pam_3CSK_4 elicited equal amounts of IgG antibodies, with ∼4-fold increase compared to S-ECD protein. These results indicate that MPLA is a promising adjuvant, which triggers stronger humoral immune responses compared to α-GalCer and Pam_3CSK_4, and that liposomes play an important role in improving immune efficacy.

We also measured IgG subtype titers to assess Th1/Th2 polarization. The IgG1 subtype is generally related to the Th2 immune response, while IgG2a and IgG2b are predominantly produced during Th1 immunity. The results showed that MPLA elicited an improved Th1/Th2 balanced immune response, as both the liposomal (Figure 3B) and nonliposomal (Figure S2D) formulations significantly increased IgG2a and IgG2b levels compared to their S-ECD controls. In contrast, Alum is a typical Th2-biased immunostimulant, which predominantly results in the production of IgG1 (Figure S2D). Therefore, it is beneficial to use MPLA as a potent adjuvant because the immune responses induced by MPLA-adjuvanted vaccines feature a broad IgG subtype distribution and, therefore, more effective protection.

Cellular Responses Induced by Vaccines Using Different Adjuvants. T-cell-mediated cellular immunity plays an essential role in the long term protection against viral infections.[36] To investigate the contribution of different adjuvants and different vaccine formulations on cellular

https://doi.org/10.1021/acs.jmedchem.1c02025
J. Med. Chem. XXXX, XXX, XXX−XXX

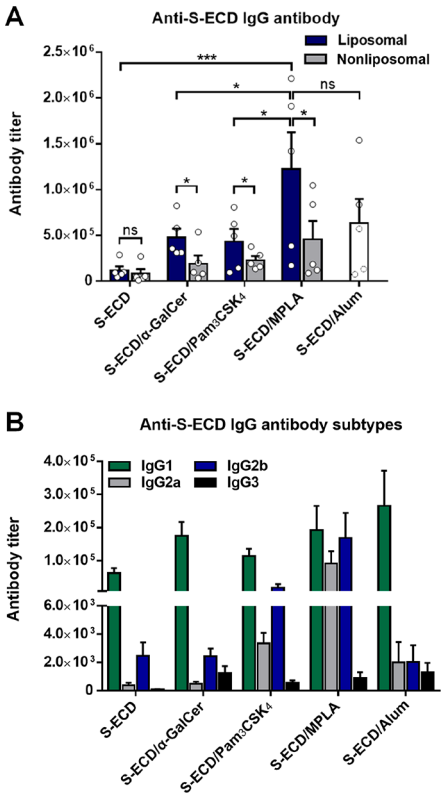

Figure 3. Specific antibody responses induced by vaccines using different adjuvants. (A) Anti-S-ECD IgG antibody titers elicited by liposomal and nonliposomal vaccines as indicated on day 42. (B) IgG antibody subtype distribution on day 42. Data are shown as the mean ± SEM of 5 mice per group and are representative of three separate experiments. Statistical significance was determined using unpaired two-tailed *t* test (for liposomal and nonliposomal samples) and one-way ANOVA with Dunn's multiple comparison test. No significant difference: ns, $P < 0.05$: *, $P < 0.01$: **, and $P < 0.001$: ***.

immunity, splenocytes were collected from vaccinated mice 2 weeks after the last injection, and the S-specific cellular responses were measured by IFN-γ ELISPOT and intracellular cytokine staining (ICS) assay. The splenocytes were stimulated with 100 μg/mL of overlapping peptide pool (spanning SARS-CoV-2 S) for 18 h before forming IFN-γ spots. As shown in Figure 4A, the liposomal groups induced more IFN-γ spots than their nonliposomal controls, and the MPLA significantly increased not only the overall antibody titers but also the number of specific IFN-γ spots compared to S-ECD alone in liposomal formulations. The S-ECD/MPLA liposome group elicited the most IFN-γ spots, but was not significantly different from the S-ECD/α-GalCer and S-ECD/Pam_3CSK_4 liposome groups. ICS assay was performed for IFN-γ- and TNF-α-secreting cells. Cytokine-producing CD4+ and CD8+ T cells in the spleen were evaluated by flow cytometry (Figure 4B,C and Figures S3 and S4). Similar to the ELISPOT results, the liposomal groups induced a higher frequency of IFN-γ- and TNF-α-producing CD4+ or CD8+ T cells than the non-liposomal groups. Meanwhile, S-ECD/MPLA liposomes induced significantly more cytokine-producing cells than the S-ECD liposomes and S-ECD plus Alum adjuvant, whereas the S-ECD/α-GalCer and S-ECD/Pam_3CSK_4 groups elicited comparable T cell responses as S-ECD alone in the liposomal and nonliposomal formulations. These results suggest that MPLA may be an efficient adjuvant for improving the T cell response against SARS-CoV-2. Collectively, the liposome has been proven to be an ideal delivery system for vaccine components, as it promotes both humoral and cellular immune responses, and MPLA is a promising adjuvant for the development of effective COVID-19 vaccine candidates.

Specific Antibody Responses Induced by MPLA-Adjuvanted Liposomal Vaccines Using Different Antigens. Although numerous vaccines based on the S protein and its subunits have been developed and extensively evaluated in animal models since the emergence of SARS-CoV-2, few studies have systematically compared the key target proteins of S protein, that is, S-trimer, S-ECD, S1, and RBD.[37] Therefore, based on the finding that the MPLA-adjuvanted liposomal vaccine induced the most potent immune responses, we further utilized this vaccine formulation to evaluate different antigen proteins, in which the antigen dose was set as 10 μg for S-trimer, S-ECD, S1, and RBD. The specific antibody responses against the corresponding antigens showed that the S-trimer/MPLA liposomes induced the highest IgG antibody titers on day 42, but there was no significant difference among the four groups (Figure 5A). Meanwhile, S-trimer/MPLA rapidly elicited a strong humoral response compared to other groups after two immunizations (Figure S5A). Interestingly, the RBD-specific antibody titers induced by S-trimer/MPLA and S-ECD/MPLA groups were significantly lower compared to those induced by S1/MPLA and RBD/MPLA groups (Figure 5B). This may be because the molar amount of RBD administered varied across different antigen proteins, as the molar amounts are different despite having the same quality. We also evaluated cross-recognition of S-trimer, S1 and S-ECD by the antibodies from S-trimer/MPLA, S1/MPLA, S-ECD/MPLA, and RBD/MPLA groups. The results showed that antibodies induced by S-ECD/MPLA almost could not recognize S-trimer, S1, and RBD proteins coated on the ELISA plates. Meanwhile, S-trimer/MPLA, S1/MPLA, and RBD/MPLA groups induced significantly lower level of anti-S-ECD antibodies than the anti-S-trimer antibodies, respectively (Figure S5B). The IgG antibody subtype distribution indicated that all groups induced Th1/Th2 balanced immunity (Figure 5C), which is in agreement with the antibody subclass profile of MPLA-adjuvanted vaccines.

Evaluation of S-Trimer, ECD, S1, and RBD for Pseudovirus Neutralizing Activity and Cross-Neutralization of Variants. The production of functional antibodies with strong viral neutralizing activity directly contributes to the protection conferred by a vaccine candidate. Therefore, the neutralizing antibody responses of each group were compared against wild-type (WT) pseudotyped SARS-CoV-2. As shown in Figure 6A, WT pseudovirus neutralization ID_{50} ($pVNT_{50}$) of mouse sera (day 42) showed that the RBD/MPLA group generated the highest neutralizing antibody activity (mean $pVNT_{50}$ = 14031), followed by the S-trimer/MPLA group (mean $pVNT_{50}$ = 11446) and the S1/MPLA group (mean $pVNT_{50}$ = 7240). Surprisingly, the S-ECD/MPLA vaccination induced a very low-level neutralizing response ($pVNT_{50} < 400$). Although S-trimer/MPLA induced a lower level of anti-RBD antibodies compared to S1/MPLA and RBD/MPLA (Figure 5B), the neutralizing antibody titer induced by S-trimer/MPLA was equivalent to that of RBD/MPLA. This suggests that the non-RBD regions can also induce neutralizing antibodies, such as the NTD and CTD (C-terminal domain) of the S protein.[38,39] These results indicate that S-trimer and RBD are more effective antigens in protecting against SARS-CoV-2 infection than ECD and that S1 is a moderately effective antigen, which is in

https://doi.org/10.1021/acs.jmedchem.1c02025
J. Med. Chem. XXXX, XXX, XXX−XXX

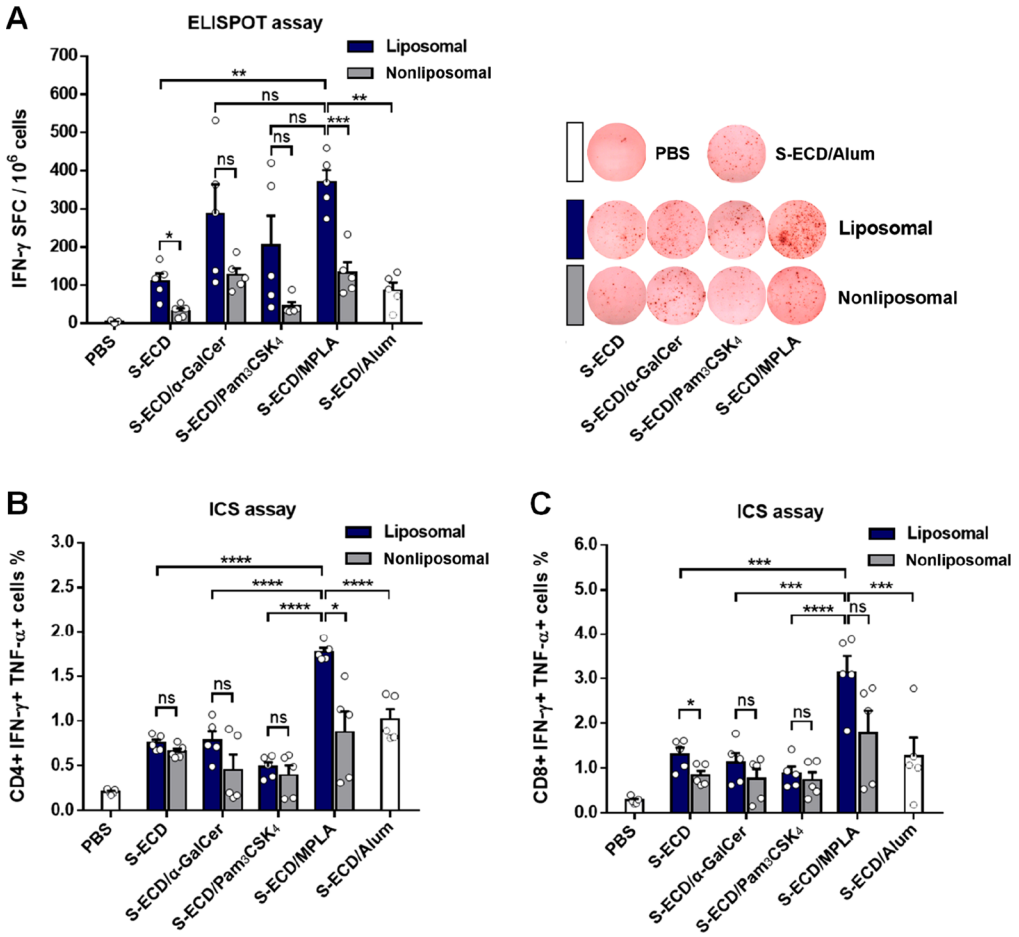

Figure 4. Specific cytokine-producing T cell immune responses induced by vaccines as indicated. Splenocytes were separated from immunized mice on day 42 and stimulated with overlapping peptide pool (spanning SARS-CoV-2-S S1 + S2) for 18 h, and cells were evaluated by ELISPOT assay (A) and flow cytometry for IFN-γ and TNF-α double positive cells in CD4+ (B) and CD8+ (C) T cells. Data are shown as the mean ± SEM of 5 mice per group; each sample was performed in triplicate. Statistical significance was determined using unpaired two-tailed *t* test (for liposomal and nonliposomal samples) and one-way ANOVA with Dunn's multiple comparison test. No significant difference: ns, $P < 0.05$: *, $P < 0.01$: **, $P < 0.001$: ***, and $P < 0.0001$: ****.

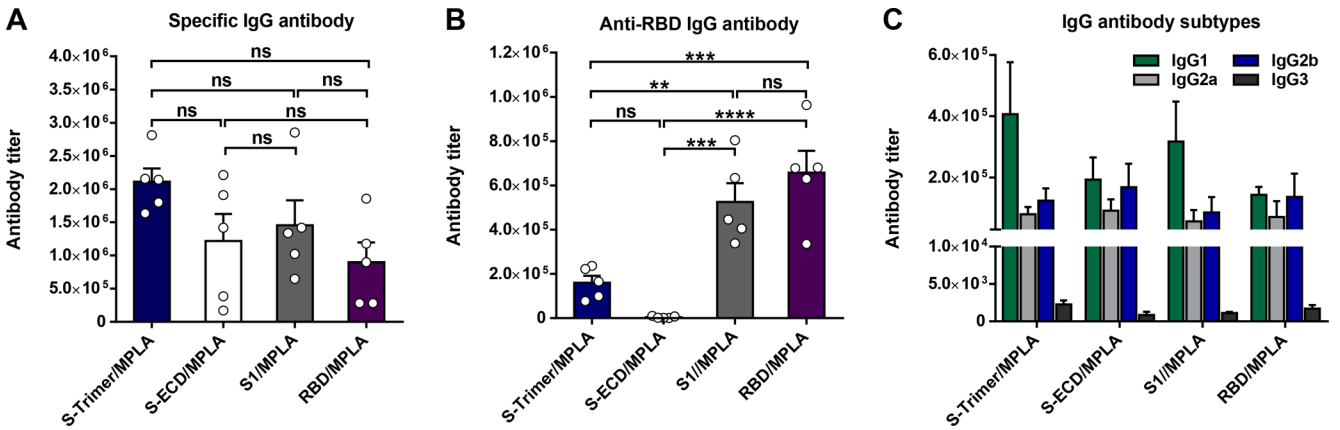

Figure 5. Specific antibody responses induced by vaccines with different antigens as indicated. (A) Specific IgG antibody titers (day 42) elicited by vaccines as indicated against their corresponding antigens. (B) Anti-RBD IgG antibody titers (day 42) measured by ELISA plates coated with RBD. (C) Subtype distribution of IgG antibody (day 42) against their corresponding antigen. The antigen and MPLA doses immunized for all groups were 10 μg and 8.8 μg per mouse, respectively. Data are shown as the mean ± SEM of 5 mice per group and are representative of three separate experiments. Statistical significance was determined using one-way ANOVA with Tukey's multiple comparison test. No significant difference: ns, $P < 0.05$: *, $P < 0.01$: **, $P < 0.001$: ***, and $P < 0.0001$: ****.

https://doi.org/10.1021/acs.jmedchem.1c02025
J. Med. Chem. XXXX, XXX, XXX−XXX

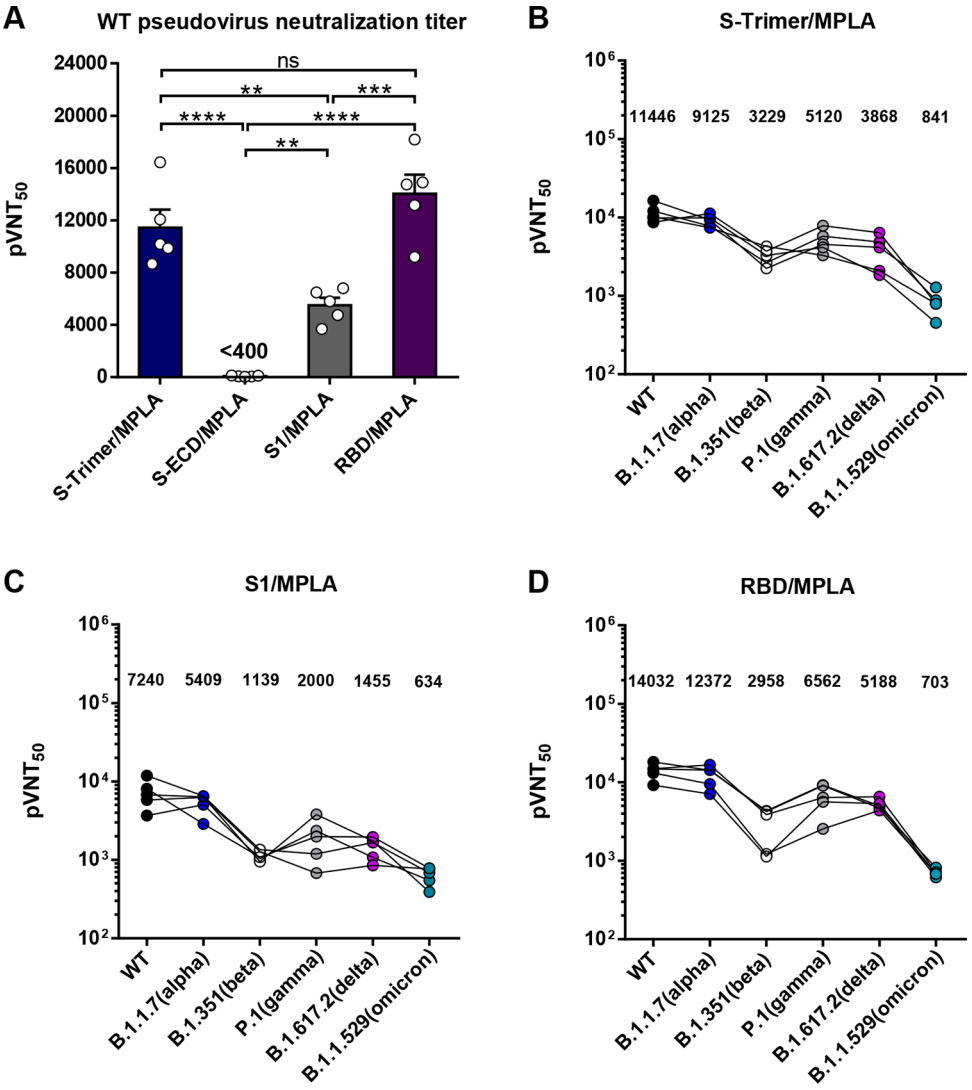

Figure 6. Neutralization of SARS-CoV-2 pseudovirus and variants by mouse sera. Mouse sera collected on day 42 were serially diluted and analyzed for neutralization. (A) Neutralization titers ($pVNT_{50}$) against WT pseudovirus. Data are shown as the mean ± SEM of $pVNT_{50}$ of 5 mice per group. Statistical significance was determined using one-way ANOVA with Tukey's multiple comparison test. No significant difference: ns, $P < 0.05$: *, $P < 0.01$: **, $P < 0.001$: ***, and $P < 0.0001$: ****. (B–D) Neutralization titers ($pVNT_{50}$) against variant pseudoviruses in the presence of serially diluted mouse sera from S-trimer/MPLA (B), S1/MPLA (C), and RBD/MPLA (D) groups. Data of a given sample for each mouse were linked to trace its neutralization titers against different pseudoviruses. Mean $pVNT_{50}$ against different variants relative to the WT are shown and compared.

accordance with the findings of previous studies.[37] Therefore, S-trimer, RBD, and S1 are likely to be superior for subunit vaccine development.

Furthermore, considering the pandemic is still ongoing with variants spreading globally, it is important to know how the vaccine candidates perform against different SARS-CoV-2 variant. The World Health Organization (WHO) has classified the variants B.1.1.7/alpha, B.1.351/beta, P.1/gamma, B.1.617.2/delta, and B.1.1.529/omicron as variants of concern (VOCs),[40] and the United States Centers for Disease Control and Prevention (CDC) has classified B.1.1.7, B.1.351, and P.1 as variants being monitored and B.1.617.2 and B.1.1.529 as VOCs.[41] Cross-neutralization of these five variants was performed to evaluate the neutralization breadth of the antisera from these liposomal vaccines containing different antigens (Figure 6B–D). The results showed that in the S-trimer/MPLA group, neutralizing antibody titers against WT and B.1.1.7 were comparable; however, neutralizing titers of S-trimer/MPLA group against B.1.351, P.1, B.1.617.2 and B.1.1.529 were 3.5-, 2.2-, 2.9- and 13.6-fold lower than that against the WT, respectively. A similar neutralization pattern was observed for the RBD/MPLA group, with a fold decrease of 4.7 for B.1.351, 2.1 for P.1, 2.7 for B.1.617.2, and 19.9 for B.1.1.529 relative to the WT. The mean $pVNT_{50}$ of the S1/MPLA group against variants was lower than those of the S-trimer/MPLA and RBD/MPLA groups, but it was still effective for the S1/MPLA group to neutralize these variants. In addition, S-ECD/MPLA showed undetectable levels of neutralization against WT or variants (data not shown). Therefore, S-trimer/MPLA, RBD/MPLA, and S1/MPLA, especially the former two, have the potential to provide effective protection against different variants emerging worldwide.

T-Cell Responses Induced by Liposomal Vaccines Using S-Trimer, S-ECD, S1, and RBD as Antigens. The T-cell immune responses induced by S-trimer/MPLA, S-ECD/MPLA, S1/MPLA, and RBD/MPLA were also measured by IFN-γ ELISPOT (Figure 7A) and ICS assay (Figure 7B,C, Figure S6). To this end, splenocytes were collected from

https://doi.org/10.1021/acs.jmedchem.1c02025
J. Med. Chem. XXXX, XXX, XXX–XXX

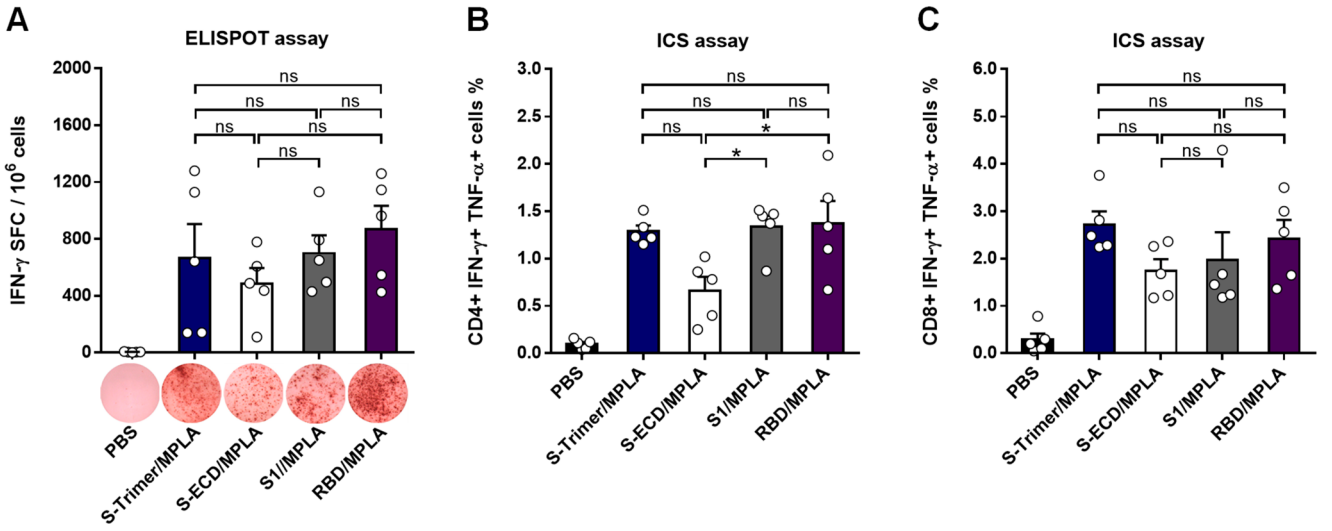

Figure 7. Specific cytokine-producing T cell immune responses induced by vaccines with different antigens. Splenocytes were separated from immunized mice on day 42 and stimulated with overlapping peptide pool (spanning SARS-CoV-2-S S1 + S2) for 18 h, and cells were evaluated by ELISPOT assay (A) and flow cytometry for IFN-γ and TNF-α double positive cells in CD4+ (B) and CD8+ (C) T cells. Data are shown as the mean ± SEM of 5 mice per group; each sample was performed in triplicate. Statistical significance was determined using one-way ANOVA with Tukey's multiple comparison test. No significant difference: ns, $P < 0.05$: *, $P < 0.01$: **, $P < 0.001$: ***, and $P < 0.0001$: ****.

immunized mice on day 42 and stimulated with 100 μg/mL of overlapping peptide pool (spanning SARS-CoV-2-S S1 + S2) for 18 h before forming IFN-γ spots. All the four vaccines induced high numbers of IFN-γ spots and cytokine-producing (IFN-γ+ TNF-α+) CD8+ T cells with no significant difference compared to each other (Figure 7A,C), although the specific cytokine-producing CD4+ T cell response induced by the S-ECD/MPLA group was relatively weak compared with other vaccines (Figure 7B). These results suggest that S-trimer, S-ECD, S1, and RBD combined with MPLA in liposomes not only induce specific antibody responses but also effective T cell immunity. Considering the poor ability of S-ECD to elicit neutralization responses, the use of S-trimer, S1, and RBD as antigens in MPLA-adjuvanted liposomes is considered a promising strategy for the provision of broad protective immunity.

DISCUSSION AND CONCLUSIONS

Careful adjuvant and antigen selection is of the utmost importance for the development of subunit vaccines. As a clinically approved adjuvant component, MPLA has been used as a potent adjuvant in subunit vaccines against SARS-CoV-2.[42,43] We have shown that MPLA-adjuvanted vaccines elicited stronger humoral and cellular immune responses than those adjuvanted by α-GalCer, Pam_3CSK_4, or even traditional Alum. Due to the amphiphilic structure of these three lipophilic adjuvants, we evaluated the liposomal and nonliposomal formulations of vaccines to optimize their immune efficiency. Compared to the simple admixture of antigen and adjuvant, liposomal formulation has superior codelivery of vaccine components, which are taken up by APCs for simultaneous stimulation with both adjuvant and antigen.[24−26] Moreover, liposomal formulations improve the solubility of lipophilic adjuvants in water.

Since the outbreak of COVID-19, extensive research conducted on SARS-CoV-2 has facilitated the rapid advancement of subunit vaccines in clinical trials.[44] Most candidates aim to provoke neutralizing antibodies against the S protein because of its key role in viral invasion. However, it is unclear how the neutralizing abilities of different forms of the S protein used in different vaccines are related to each other. Herein, we systematically compared S-trimer, S-ECD, S1, and RBD as antigens in MPLA-adjuvanted liposomal vaccines. The results showed that all four antigens could induce strong specific antibody responses (Figure 5A), but only S-trimer, S1, and RBD elicited substantial neutralizing antibody titers. The extent of neutralizing ability induced by these four antigens was RBD > S-trimer > S1 ≫ S-ECD (Figure 6A). Like other type 1 fusion proteins, S protein undergoes a conformational rearrangement when binding to the ACE2, which destabilizes the S prefusion state and triggers the transition into the postfusion conformation (Figure 1C). Although a tiny percentage of S protein can spontaneously refold to the postfusion conformation independent of target cells, the S-trimer predominately adopts the prefusion state as a stable conformation. Notably, the irreversible transition to the postfusion form would disrupt the prefusion-specific antigenic epitopes on S protein and reduce its ability to induce neutralizing antibodies.[4,5,45−48] As S-ECD monomer is less stable than S-trimer, which is tightly packed among the three monomers, it would be difficult for S-ECD to maintain the prefusion form, thereby leading to its failure to induce effective neutralizing antibodies. In addition, studies have shown that most SARS-CoV-2 RBD-specific neutralizing antibodies recognize conformational, but not linear, epitopes.[49,50] Therefore, the instability of S-ECD and the consequent structural changes might account for that S-ECD-induced antibodies lost the ability to recognize the S-trimer, S1, and RBD proteins (Figure 5B, Figure S5B). Therefore, S-ECD would not be considered an appropriate antigen in meeting the challenge of protection against viral infections. In contrast, at the same antigen dose, S-trimer and RBD are optimal antigens for subunit vaccine development, with superior immunogenicity compared to S-ECD, while S1 is a moderate optimal antigen for subunit vaccine development.

As SARS-CoV-2 evolves and new variants emerge worldwide, the assessment of variant cross-neutralization induced by a new vaccine candidate is necessary for broad protection. Studies have reported that antibody responses triggered by infection or vaccination might effectively neutralize variant B.1.1.7 (alpha),

https://doi.org/10.1021/acs.jmedchem.1c02025
J. Med. Chem. XXXX, XXX, XXX−XXX

but that neutralizing titers against B.1.351 (beta), P.1 (gamma), B.1.617.2 (delta), and B.1.1.529 (omicron) suffered large reductions, among which the omicron variant exhibited the greatest magnitude of immune evasion from the neutralizing antbodies.[51−54] The results of cross-neutralization against five variants showed that, with the exception of S-ECD/MPLA, S-trimer/MPLA, S1/MPLA, and RBD/MPLA groups effectively neutralized these variants. Together with the neutralization ability against the WT, S-trimer, RBD, and S1, especially S-trimer and RBD, would represent ideal choices for designing an effective vaccine with broad protection.

In summary, we investigated the effect of liposome formulation, adjuvant choice, and antigen selection on the immune responses and compared the neutralizing ability elicited by liposomes encapsulating different subunits of S protein. MPLA-adjuvanted liposomes, which elicit potent humoral and cellular immune responses, provide a facile method to prepare effective COVID-19 vaccines. Most importantly, S-trimer/MPLA and RBD/MPLA liposomes showed striking neutralization efficiency against SARS-CoV-2, compared to S1/MPLA and S-ECD/MPLA, which elicited moderate and minor neutralization, respectively. Moreover, antibodies induced by S-trimer/MPLA, RBD/MPLA, and S1/MPLA remain effective against spike variants, including B.1.1.7/alpha, B.1.351/beta, P.1/gamma, B.1.617.2/delta, and B.1.1.529/omicron. Therefore, due to the weakness of eliciting neutralizing responses, S-ECD adjuvanted with MPLA in liposome is not considered appropriate for subunit vaccine design. In contrast, MPLA-adjuvanted liposomes encapsulating S-trimer, RBD, or S1 provide strong potential to address the clinical challenges of SARS-CoV-2 and variant infections. We expect that this promising vaccine platform will contribute to the international effort toward vaccines against SARS-CoV-2 and its circulating variants and the possible outbreak of other types of coronaviruses in the future.

EXPERIMENTAL SECTION

Materials and Reagents. MPLA was purchased from Sigma-Aldrich (Avanti Polar Lipids, Alabaster, AL, USA). α-GalCer[32,55] and Pam_3CSK_4[24] were prepared according to our previously reported procedures. 1,2-Distearoyl-*sn*-glycero-3-phosphocholine (DSPC) was purchased from TCI. Cholesterol was purchased from Energy Chemical. Peroxidase-conjugated AffiniPure goat antimouse kappa, IgG1, IgG2a, IgG2b, and IgG3 antibodies were purchased from Southern Biotechnology, and peroxidase-conjugated AffiniPure goat antimouse kappa antibodies IgG and IgM were purchased from Jackson ImmunoResearch. Reagents used were RPMI1640, DMEM, and fetal bovine serum (FBS) (Gibco). Bovine serum albumin (BSA) and Alum adjuvant (Alum) were purchased from Thermo Fisher Scientific. The bicichonic acid (BCA) protein assay kit was purchased from Elabscience (Wuhan, China). The SARS-CoV-2 spike ECD protein (S1 + S2, His tag) was purchased from SinoBiological (40589-V08B1). S-trimer (His tag, VISC2-S02), S1 (His tag, VISC2-S1), and RBD (His tag, VISC2-RB04) proteins were provided by Jiangsu East-mab Biomedical Technology. All animal experiments were performed at Laboratory Animal Centre of Huazhong Agricultural University (Wuhan, China). Animal experiments were conducted according to the animal ethics guidelines and follow the recommendations concerning laboratory animal welfare.

Vaccination. Thirteen groups of female BALB/c mice (n = 5/group, 6−8 weeks old) were immunized subcutaneously three times at 2-week intervals. Groups 1−4 were administered with liposomes containing 10 μg of S-ECD protein alone or plus 2 μg of α-GalCer, 7.5 μg of Pam_3CSK_4 and 8.8 μg of MPLA, respectively, and groups 5−8 were vaccinated with the same doses of antigen and adjuvant in nonliposomal formulation. Group 9 was immunized with 10 μg of S-ECD protein plus 100 μL of Alum. Groups 10−13 were immunized with 8.8 μg of MPLA plus 10 μg of S-trimer, S-ECD, S1, and RBD, respectively, in liposomal formulation.

Preparation of Liposomal Vaccines. Liposomes were prepared following previously reported protocols.[24,32] A mixture of DSPC (33.27 μg for one dose), cholesterol (8.14 μg for one dose), and lipophilic adjuvants (2 μg of α-GalCer, 7.5 μg of Pam_3CSK_4, or 8.8 μg of MPLA for one dose) were dissolved in 2 mL of CH_2Cl_2/MeOH (1:1, v/v). The solvents were removed under reduced pressure through evaporation, which generated a thin lipid film on the flask wall. Then antigen proteins (10 μg of S-ECD, S-trimer, S1, or RBD for one dose) were added in the flask followed by overnight freeze-drying. Next, 1.2 mL of PBS (pH 7.4) was added to hydrate the film, which was finally sonicated for 10 min and injected in mice immediately. The molar ratio of DSPC:cholesterol:adjuvant is 8:4:1 for S-ECD/MPLA, S-trimer/MPLA, S1/MPLA, RBD/MPLA, and S-ECD/Pam_3CSK_4 groups and 8:4:0.47 for the S-ECD/α-GalCer group.

Physicochemical Characterization of Liposomes. The liposomes mean diameter were determined by DLS (Zetasizer Nano ZS, Malvern Instruments, UK). The ζ potential was measured by laser doppler electrophoresis (Malvern Instruments, Worcestershire, UK). All the measurements were determined at room temperature (rt) in triplicate.

After liposome preparation, the liposomes were centrifugated at 12000*g* for 60 min. The top supernatant was carefully transferred, and the concentration of nonencapsulated protein was determined using a micro-BCA protein assay kit according to the manufacturer's instructions for 96-microwell plates (Costar type 3590, Corning Inc.). The absorbance of samples was measured at 562 nm using a microplate reader (BioTek Instruments, Synergy H1, USA). The entrapment efficiency (EE) was calculated according to the following equation (for results, see Table S1):

$$\mathrm{EE}\,(\%) = \frac{W_{\mathrm{total}} - W_{\mathrm{free}}}{W_{\mathrm{total}}} \times 100\%$$

where W_{total} and W_{free} represent the weights of the total and nonencapsulated protein, respectively.

Analysis of Antibody Titers and Subtypes by ELISA. Antibody titers and subtypes were measured by ELISA. Antigen protein was dissolved in the prepared $NaHCO_3/Na_2CO_3$ buffer (50 mM, pH 9.5) with the final concentration of 1 μg/mL. Next, 96-well plates (Costar type 3590, Corning Inc.) were coated with the antigen protein at 4 °C overnight. Then, the coated plates were washed three times with PBST (PBS + 0.1% Tween) and blocked with 2% BSA in PBS (100 μL/well) at 37 °C for 1 h. After washing three times, the plates were incubated with the serially diluted sera samples in PBS containing 0.1% BSA (100 μL/well) at 37 °C for 1 h. After another washing step, the plates were incubated with one of the HRP-linked goat antimouse antibody IgG, IgM, IgG1, IgG2a, IgG2b, or IgG3, 1:5000 dilution in PBST (100 μL/well) at 37 °C for 1 h. After the final washing steps, TMB (500 μL, 0.2 mg/mL) in 9.5 mL of 0.05 M phosphate-citrate buffer at pH 5.0 with 32 μL 3% (w/v) urea hydrogen peroxide was added and allowed to react for 5 min in the dark. Next, the colorimetric reactions were terminated by 2.0 M H_2SO_4. Absorbance was recorded at 450 nm with a microplate reader (BioTek Instruments, Synergy H1, USA). The antibody titer was defined as the highest dilution showing an absorbance of 0.1, after subtracting the background.

ELISPOT Assay. IFN-γ secreting cells of splenocytes from each immunized group 2 weeks after the last boost were detected by IFN-γ ELISPOT kits (DAKEWE, 2210006) according to manufacture instructions. The 96-well plates were precoated with rat antimouse IFN-γ. 200 μL of RPMI1640 without FBS was added to each well to activate the monoclonal antibodies. Splenocytes harvested from vaccinated mice were seeded into the wells (1×10^6 cells/well) in RPMI 1640 with 10% (v/v) FBS, 100 U/mL penicillin, and 100 μg/mL streptomycin containing 100 μg/mL of two peptide pools (pool 1: peptides 1−158 and pool 2: peptides 159−316) consisting of a total of 316 15-mers peptides overlapping by 11 amino acids together covering the full-length spike protein in duplicate (GenScript, RP30020). The

https://doi.org/10.1021/acs.jmedchem.1c02025
J. Med. Chem. XXXX, XXX, XXX−XXX

cells were first cultured for 18 h at 37 °C 5% CO_2 and then lysed with distilled H_2O for 10 min at 4 °C. After washing the plates six times, biotinylated antimouse IFN-γ antibodies (1:100) were added and incubated for 1 h at 37 °C. After another washing step, the plates were incubated with streptavidin-HRP (1:100) for additional 1 h. After final washing steps, AEC substrate was added 100 μL per well to develop spots in dark for 30 min at rt, then the reaction was quenched with distilled H_2O, and plates were air-dried before counted.

Intracellular Cytokine Staining and Flow Cytometry. Mouse splenocytes were added to 24-well plates at 10^6 cells per well. The cells were stimulated with two peptide pools (pool 1: peptides 1−158 and pool 2: peptides 159−316) consisting of a total of 316 15-mers peptides overlapping by 11 amino acids together covering the full-length spike protein for 3 h. Next, monensin and brefeldin A (BD Biosciences) were added to block the protein transport, and the plates were incubated at 37 °C for 15 h. Cells were collected by centrifugation and stained with anti-CD3, anti-CD4, and anti-CD8 markers (BioLegend) for 30 min on ice. After washing, the cells were fixed, permeabilized, and stained with anti-TNF-α and anti-IFN-γ markers (BioLegend) for 30 min on ice. Cells were analyzed with a CytoFLEX S flow cytometer (Beckman Coulter).

Pseudovirus Neutralization Assay. Pseudovirus neutralization assay was performed using lentivirus-based SARS-CoV-2 pseudoviruses bearing WT (Genomeditech, GM-0220PV07) and B.1.1.7 (Genomeditech, GM-0220PV33), B.1.351 (Genomeditech, GM-0220PV32), P.1 (Genomeditech, GM-0220PV47), B.1.617.2 (Genomeditech, GM-0220PV45), and B.1.1.529 (Genomeditech, GM-0220PV84) variants spike protein. Briefly, mouse sera was preheated at 56 °C for 30 min and serially diluted before incubating with 2×10^4 $TCID_{50}$ pseudoviruses for 1 h at rt in duplicate. The mixture was added to 2×10^4 HEK293T-ACE2 cells (Genomeditech, GM-C09233) per well and incubated for 48 h of incubation in 5% CO_2 environment at 37 °C. The luminescence was measured using Biolite Luciferase assay system (Genomeditech, G0483M001 and G0483M002) and detected for relative light units (RLUs) using a microplate reader (BioTek Instruments, Synergy H1, USA). The titer of neutralization antibody ($pVNT_{50}$) was defined as the reciprocal serum dilution at which the RLUs were reduced by 50% compared to the virus control wells (virus + cells) after subtraction of background RLUs in the control groups with cells only.

Statistical Analyses. Comparison of multiple groups for statistical significance was carried out via one-way ANOVA with Dunn's or Tukey's multiple comparison test. Statistically significant responses are indicated by asterisks. A P-value $\leqslant 0.05$ was considered statistically significant. Data were analyzed using GraphPad Prism (GraphPad Software, San Diego, CA). Flow cytometry data was analyzed with the Cytexpert 2.4 software.

■ ASSOCIATED CONTENT

Supporting Information

The Supporting Information is available free of charge at https://pubs.acs.org/doi/10.1021/acs.jmedchem.1c02025.

Characterization of vaccine liposomes; S-ECD-specific IgG antibody titers measured by ELISA; example flow cytometry plots for CD4+ and CD8+ T cells expressing IFN-γ and TNF-α; specific IgG antibody titers elicited by vaccines against corresponding antigens (PDF)

■ AUTHOR INFORMATION

Corresponding Author

Jun Guo − *Key Laboratory of Pesticide and Chemical Biology of Ministry of Education, International Joint Research Center for Intelligent Biosensing Technology and Health, Hubei International Scientific and Technological Cooperation Base of Pesticide and Green Synthesis, College of Chemistry, Central China Normal University, Wuhan 430079, China;* orcid.org/0000-0002-2097-5054; Email: jguo@mail.ccnu.edu.cn

Authors

Jian Wang − *Key Laboratory of Pesticide and Chemical Biology of Ministry of Education, International Joint Research Center for Intelligent Biosensing Technology and Health, Hubei International Scientific and Technological Cooperation Base of Pesticide and Green Synthesis, College of Chemistry, Central China Normal University, Wuhan 430079, China*

Xu-Guang Yin − *School of Medical Sciences, Shaoxing University, Zhejiang 312000, China*

Yu Wen − *Key Laboratory of Pesticide and Chemical Biology of Ministry of Education, International Joint Research Center for Intelligent Biosensing Technology and Health, Hubei International Scientific and Technological Cooperation Base of Pesticide and Green Synthesis, College of Chemistry, Central China Normal University, Wuhan 430079, China*

Jie Lu − *Key Laboratory of Pesticide and Chemical Biology of Ministry of Education, International Joint Research Center for Intelligent Biosensing Technology and Health, Hubei International Scientific and Technological Cooperation Base of Pesticide and Green Synthesis, College of Chemistry, Central China Normal University, Wuhan 430079, China*

Ru-Yan Zhang − *Key Laboratory of Pesticide and Chemical Biology of Ministry of Education, International Joint Research Center for Intelligent Biosensing Technology and Health, Hubei International Scientific and Technological Cooperation Base of Pesticide and Green Synthesis, College of Chemistry, Central China Normal University, Wuhan 430079, China*

Shi-Hao Zhou − *Key Laboratory of Pesticide and Chemical Biology of Ministry of Education, International Joint Research Center for Intelligent Biosensing Technology and Health, Hubei International Scientific and Technological Cooperation Base of Pesticide and Green Synthesis, College of Chemistry, Central China Normal University, Wuhan 430079, China*

Chun-Miao Liao − *Key Laboratory of Pesticide and Chemical Biology of Ministry of Education, International Joint Research Center for Intelligent Biosensing Technology and Health, Hubei International Scientific and Technological Cooperation Base of Pesticide and Green Synthesis, College of Chemistry, Central China Normal University, Wuhan 430079, China*

Hua-Wei Wei − *Jiangsu East-Mab Biomedical Technology Co. Ltd, Nantong 226499, China*

Complete contact information is available at: https://pubs.acs.org/10.1021/acs.jmedchem.1c02025

Author Contributions

‖These authors contributed equally.

Funding

This work was supported by the National Natural Science Foundation of China (21772056 and 22177035), the National Key Research and Development Program of China (2017YFA0505200), Wuhan Bureau of Science and Technology (2020020601012217), the self-determined research funds of CCNU from the colleges' basic research and operation of MOE (CCNU20TS016), and Program of Introducing Talents of Discipline to Universities of China (111 program, B17019).

Notes

The authors declare no competing financial interest.

■ ABBREVIATIONS USED

SARS-CoV-2, severe acute respiratory syndrome coronavirus 2; COVID-19, coronavirus disease 2019; MERS-CoV, Middle East respiratory syndrome coronavirus; RBD, receptor-binding

domain; ACE2, angiotensin-converting enzyme 2; S-ECD, S protein extracellular domain; α-GalCer, α-galactosylceramide; iNKT, invariant natural killer T; TLR, toll-like receptor; MPLA, monophosphoryl lipid A; DC, dendritic cell; VOC, variant of concern; WT, wild-type; DSPC, 1,2-distearoyl-*sn*-glycero-3-phosphocholine; APCs, antigen-presenting cells; ELISA, enzyme-linked immunosorbent assay; BSA, bovine serum albumin; FBS, fetal serum albumin; ICS, intracellular cytokine staining; PBS, phosphate-buffered saline; SEM, standard error of measurement; NTD, the N-terminal domain; CTD, the C-terminal domain; EE, encapsulation efficiency; DLS, dynamic light scattering; BCA, bicinchonic acid

REFERENCES

(1) V'Kovski, P.; Kratzel, A.; Steiner, S.; Stalder, H.; Thiel, V. Coronavirus biology and replication: implications for SARS-CoV-2. *Nat. Rev. Microbiol.* **2021**, *19* (3), 155−170.

(2) Hoffmann, M.; Kleine-Weber, H.; Schroeder, S.; Kruger, N.; Herrler, T.; Erichsen, S.; Schiergens, T. S.; Herrler, G.; Wu, N. H.; Nitsche, A.; Muller, M. A.; Drosten, C.; Pohlmann, S. SARS-CoV-2 cell entry depends on ACE2 and TMPRSS2 and is blocked by a clinically proven protease inhibitor. *Cell* **2020**, *181* (2), 271−280.

(3) Ye, F.; Zhao, J.; Xu, P.; Liu, X.; Yu, J.; Shangguan, W.; Liu, J.; Luo, X.; Li, C.; Ying, T.; Wang, J.; Yu, B.; Wang, P. Synthetic homogeneous glycoforms of the SARS-CoV-2 spike receptor-binding domain reveals different binding profiles of monoclonal antibodies. *Angew. Chem. Int.* **2021**, *60*, 12904−12910.

(4) Bangaru, S.; Ozorowski, G.; Turner, H. L.; Antanasijevic, A.; Huang, D. L.; Wang, X. N.; Torres, J. L.; Diedrich, J. K.; Tian, J. H.; Portnoff, A. D.; Patel, N.; Massare, M. J.; Yates, J. R.; Nemazee, D.; Paulson, J. C.; Glenn, G.; Smith, G.; Ward, A. B. Structural analysis of full-length SARS-CoV-2 spike protein from an advanced vaccine candidate. *Science* **2020**, *370*, 1089−1094.

(5) Wrapp, D.; Wang, N. S.; Corbett, K. S.; Goldsmith, J. A.; Hsieh, C. L.; Abiona, O.; Graham, B. S.; McLellan, J. S. Cryo-EM structure of the 2019-nCoV spike in the prefusion conformation. *Science* **2020**, *367*, 1260−1263.

(6) Powell, A. E.; Zhang, K.; Sanyal, M.; Tang, S.; Weidenbacher, P. A.; Li, S.; Pham, T. D.; Pak, J. E.; Chiu, W.; Kim, P. S. A single immunization with spike-functionalized ferritin vaccines elicits neutralizing antibody responses against SARS-CoV-2 in mice. *ACS Cent. Sci.* **2021**, *7* (1), 183−199.

(7) Liang, J. G.; Su, D.; Song, T. Z.; Zeng, Y.; Huang, W.; Wu, J.; Xu, R.; Luo, P.; Yang, X.; Zhang, X.; Luo, S.; Liang, Y.; Li, X.; Huang, J.; Wang, Q.; Huang, X.; Xu, Q.; Luo, M.; Huang, A.; Luo, D.; Zhao, C.; Yang, F.; Han, J. B.; Zheng, Y. T.; Liang, P. S-Trimer, a COVID-19 subunit vaccine candidate, induces protective immunity in nonhuman primates. *Nat. Commun.* **2021**, *12* (1), 1346.

(8) Wu, J. J.; Zhao, L.; Han, B. B.; Hu, H. G.; Zhang, B. D.; Li, W. H.; Chen, Y. X.; Li, Y. M. A novel STING agonist for cancer immunotherapy and a SARS-CoV-2 vaccine adjuvant. *Chem. Commun.* **2021**, *57* (4), 504−507.

(9) Liu, L.; Liu, Z.; Chen, H.; Liu, H.; Gao, Q.; Cong, F.; Gao, G.; Chen, Y. Subunit nanovaccine with potent cellular and mucosal immunity for COVID-19. *ACS Applied Bio. Materials* **2020**, *3* (9), 5633−5638.

(10) He, C.; Yang, J.; He, X.; Hong, W.; Lei, H.; Chen, Z.; Shen, G.; Yang, L.; Li, J.; Wang, Z.; Song, X.; Wang, W.; Lu, G.; Wei, X. A bivalent recombinant vaccine targeting the S1 protein induces neutralizing antibodies against both SARS-CoV-2 variants and wild-type of the virus. *MedComm.* **2021**, *2*, 430−441.

(11) Yang, J.; Wang, W.; Chen, Z.; Lu, S.; Yang, F.; Bi, Z.; Bao, L.; Mo, F.; Li, X.; Huang, Y.; Hong, W.; Yang, Y.; Zhao, Y.; Ye, F.; Lin, S.; Deng, W.; Chen, H.; Lei, H.; Zhang, Z.; Luo, M.; Gao, H.; Zheng, Y.; Gong, Y.; Jiang, X.; Xu, Y.; Lv, Q.; Li, D.; Wang, M.; Li, F.; Wang, S.; Wang, G.; Yu, P.; Qu, Y.; Yang, L.; Deng, H.; Tong, A.; Li, J.; Wang, Z.; Yang, J.; Shen, G.; Zhao, Z.; Li, Y.; Luo, J.; Liu, H.; Yu, W.; Yang, M.; Xu, J.; Wang, J.; Li, H.; Wang, H.; Kuang, D.; Lin, P.; Hu, Z.; Guo, W.; Cheng, W.; He, Y.; Song, X.; Chen, C.; Xue, Z.; Yao, S.; Chen, L.; Ma, X.; Chen, S.; Gou, M.; Huang, W.; Wang, Y.; Fan, C.; Tian, Z.; Shi, M.; Wang, F. S.; Dai, L.; Wu, M.; Li, G.; Wang, G.; Peng, Y.; Qian, Z.; Huang, C.; Lau, J. Y.; Yang, Z.; Wei, Y.; Cen, X.; Peng, X.; Qin, C.; Zhang, K.; Lu, G.; Wei, X. A vaccine targeting the RBD of the S protein of SARS-CoV-2 induces protective immunity. *Nature* **2020**, *586* (7830), 572−577.

(12) Dai, L.; Zheng, T.; Xu, K.; Han, Y.; Xu, L.; Huang, E.; An, Y.; Cheng, Y.; Li, S.; Liu, M.; Yang, M.; Li, Y.; Cheng, H.; Yuan, Y.; Zhang, W.; Ke, C.; Wong, G.; Qi, J.; Qin, C.; Yan, J.; Gao, G. F. A universal design of betacoronavirus vaccines against COVID-19, MERS and SARS. *Cell* **2020**, *182* (3), 722−733.

(13) Wang, J.; Wen, Y.; Zhou, S. H.; Zhang, H. W.; Peng, X. Q.; Zhang, R. Y.; Yin, X. G.; Qiu, H.; Gong, R.; Yang, G. F.; Guo, J. Self-adjuvanting lipoprotein conjugate αGalCer-RBD induces potent immunity against SARS-CoV-2 and variants of concern. *J. Med. Chem.* **2022**, DOI: 10.1021/acs.jmedchem.1c02000.

(14) Zhou, S. H.; Zhang, R. Y.; Zhang, H. W.; Liu, Y. L.; Wen, Y.; Wang, J.; Li, Y. T.; You, Z. W.; Yin, X. G.; Qiu, H.; Gong, R.; Yang, G. F.; Guo, J. RBD conjugate vaccine with a built-in TLR1/2 agonist is highly immunogenic against SARS-CoV-2 and variants of concern. *Chem. Commun.* **2022**, DOI: 10.1039/D1CC06520C.

(15) Bok, K.; Sitar, S.; Graham, B. S.; Mascola, J. R. Accelerated COVID-19 vaccine development: milestones, lessons and prospects. *Immunity* **2021**, *54* (8), 1636−1651.

(16) Gao, J.; Guo, Z. Progress in the synthesis and biological evaluation of lipid A and its derivatives. *Med. Res. Rev.* **2018**, *38* (2), 556−601.

(17) Del Giudice, G.; Rappuoli, R.; Didierlaurent, A. M. Correlates of adjuvanticity: a review on adjuvants in licensed vaccines. *Semin. Immunol.* **2018**, *39*, 14−21.

(18) Manabe, Y.; Chang, T. C.; Fukase, K. Recent advances in self-adjuvanting glycoconjugate vaccines. *Drug Discovery Today Technol.* **2020**, *37*, 61−71.

(19) Jin, M. S.; Kim, S. E.; Heo, J. Y.; Lee, M. E.; Kim, H. M.; Paik, S. G.; Lee, H.; Lee, J. O. Crystal structure of the TLR1-TLR2 heterodimer induced by binding of a tri-acylated lipopeptide. *Cell* **2007**, *130* (6), 1071−1082.

(20) Lee, S. K.; Chwee, J. Y.; Ma, C. A.; Le Bert, N.; Huang, C. W.; Gasser, S. Synergistic anticancer effects of Pam3CSK4 and Ara-C on B-cell lymphoma cells. *Clin. Cancer Res.* **2014**, *20* (13), 3485−3495.

(21) Laurent, X.; Bertin, B.; Renault, N.; Farce, A.; Speca, S.; Milhomme, O.; Millet, R.; Desreumaux, P.; Henon, E.; Chavatte, P. Switching invariant natural killer T (iNKT) cell response from anticancerous to anti-inflammatory effect: molecular bases. *J. Med. Chem.* **2014**, *57* (13), 5489−5508.

(22) Liu, Z.; Guo, J. NKT-cell glycolipid agonist as adjuvant in synthetic vaccine. *Carbohydr. Res.* **2017**, *452*, 78−90.

(23) HogenEsch, H.; O'Hagan, D. T.; Fox, C. B. Optimizing the utilization of aluminum adjuvants in vaccines: you might just get what you want. *NPJ. Vaccines* **2018**, *3*, 51.

(24) Du, J. J.; Zou, S. Y.; Chen, X. Z.; Xu, W. B.; Wang, C. W.; Zhang, L.; Tang, Y. K.; Zhou, S. H.; Wang, J.; Yin, X. G.; Gao, X. F.; Liu, Z.; Guo, J. Liposomal antitumor vaccines targeting mucin 1 elicit a lipid-dependent immunodominant response. *Chem.—Asian J.* **2019**, *14* (12), 2116−2121.

(25) Chauhan, G.; Madou, M. J.; Kalra, S.; Chopra, V.; Ghosh, D.; Martinez-Chapa, S. O. Nanotechnology for COVID-19: therapeutics and vaccine research. *ACS Nano* **2020**, *14* (7), 7760−7782.

(26) Antimisiaris, S. G.; Marazioti, A.; Kannavou, M.; Natsaridis, E.; Gkartziou, F.; Kogkos, G.; Mourtas, S. Overcoming barriers by local drug delivery with liposomes. *Adv. Drug Delivery Rev.* **2021**, *174*, 53−86.

(27) Erikci, E.; Gursel, M.; Gursel, I. Differential immune activation following encapsulation of immunostimulatory CpG oligodeoxynucleotide in nanoliposomes. *Biomaterials* **2011**, *32* (6), 1715−1723.

(28) Bo, R.; Sun, Y.; Zhou, S.; Ou, N.; Gu, P.; Liu, Z.; Hu, Y.; Liu, J.; Wang, D. Simple nanoliposomes encapsulating Lycium barbarum polysaccharides as adjuvants improve humoral and cellular immunity in mice. *Int. J. Nanomedicine* **2017**, *12*, 6289−6301.

https://doi.org/10.1021/acs.jmedchem.1c02025
J. Med. Chem. XXXX, XXX, XXX−XXX

(29) Zhang, X. P.; Li, Y. D.; Luo, L. L.; Liu, Y. Q.; Li, Y.; Guo, C.; Li, Z. D.; Xie, X. R.; Song, H. X.; Yang, L. P.; Sun, S. B.; An, F. Y. Astragalus saponins and liposome constitute an efficacious adjuvant formulation for cancer vaccines. *Cancer Biother. Radiopharm.* **2018**, *33* (1), 25−31.
(30) Kocabas, B. B.; Almacioglu, K.; Bulut, E. A.; Gucluler, G.; Tincer, G.; Bayik, D.; Gursel, M.; Gursel, I. Dual-adjuvant effect of pH-sensitive liposomes loaded with STING and TLR9 agonists regress tumor development by enhancing Th1 immune response. *J. Controlled Release* **2020**, *328*, 587−595.
(31) Hennessy, E. J.; Parker, A. E.; O'Neill, L. A. Targeting Toll-like receptors: emerging therapeutics? *Nat. Rev. Drug Discovery* **2010**, *9* (4), 293−307.
(32) Yin, X. G.; Chen, X. Z.; Sun, W. M.; Geng, X. S.; Zhang, X. K.; Wang, J.; Ji, P. P.; Zhou, Z. Y.; Baek, D. J.; Yang, G. F.; Liu, Z.; Guo, J. IgG antibody response elicited by a fully synthetic two-component carbohydrate-based cancer vaccine candidate with alpha-galactosylceramide as built-in adjuvant. *Org. Lett.* **2017**, *19* (3), 456−459.
(33) Yin, X. G.; Lu, J.; Wang, J.; Zhang, R. Y.; Wang, X. F.; Liao, C. M.; Liu, X. P.; Liu, Z.; Guo, J. Synthesis and evaluation of liposomal anti-GM3 cancer vaccine candidates covalently and noncovalently adjuvanted by alphaGalCer. *J. Med. Chem.* **2021**, *64* (4), 1951−1965.
(34) Parekh, V. V.; Wilson, M. T.; Olivares-Villagomez, D.; Singh, A. K.; Wu, L.; Wang, C. R.; Joyce, S.; Van Kaer, L. Glycolipid antigen induces long-term natural killer T cell anergy in mice. *J. Clin. Invest.* **2005**, *115* (9), 2572−2583.
(35) Aiga, T.; Manabe, Y.; Ito, K.; Chang, T. C.; Kabayama, K.; Ohshima, S.; Kametani, Y.; Miura, A.; Furukawa, H.; Inaba, H.; Matsuura, K.; Fukase, K. Immunological evaluation of co-assembling a lipidated peptide antigen and lipophilic adjuvants: self-adjuvanting anti-breast-cancer vaccine candidates. *Angew. Chem., Int. Ed.* **2020**, *59* (40), 17705−17711.
(36) Bonifacius, A.; Tischer-Zimmermann, S.; Dragon, A. C.; Gussarow, D.; Vogel, A.; Krettek, U.; Godecke, N.; Yilmaz, M.; Kraft, A. R. M.; Hoeper, M. M.; Pink, I.; Schmidt, J. J.; Li, Y.; Welte, T.; Maecker-Kolhoff, B.; Martens, J.; Berger, M. M.; Lobenwein, C.; Stankov, M. V.; Cornberg, M.; David, S.; Behrens, G. M. N.; Witzke, O.; Blasczyk, R.; Eiz-Vesper, B. COVID-19 immune signatures reveal stable antiviral T cell function despite declining humoral responses. *Immunity* **2021**, *54* (2), 340−354.
(37) Yang, Y.; Zang, J.; Xu, S.; Zhang, X.; Yuan, S.; Wang, H.; Lavillette, D.; Zhang, C.; Huang, Z. Elicitation of broadly neutralizing antibodies against B.1.1.7, B.1.351 and B.1.617.1 SARS-CoV-2 variants by three prototype strain-derived recombinant protein vaccines. *Viruses* **2021**, *13*, 1421.
(38) Suryadevara, N.; Shrihari, S.; Gilchuk, P.; VanBlargan, L. A.; Binshtein, E.; Zost, S. J.; Nargi, R. S.; Sutton, R. E.; Winkler, E. S.; Chen, E. C.; Fouch, M. E.; Davidson, E.; Doranz, B. J.; Chen, R. E.; Shi, P. Y.; Carnahan, R. H.; Thackray, L. B.; Diamond, M. S.; Crowe, J. E., Jr. Neutralizing and protective human monoclonal antibodies recognizing the N-terminal domain of the SARS-CoV-2 spike protein. *Cell* **2021**, *184* (9), 2316−2331.
(39) Tong, J.; Zhu, C.; Lai, H.; Feng, C.; Zhou, D. Potent neutralization antibodies induced by a recombinant trimeric spike protein vaccine candidate containing PIKA adjuvant for COVID-19. *Vaccines* **2021**, *9* (3), 296.
(40) WHO *SARS-CoV-2 variants, working definitions and actions taken*, 2021. https://www.who.int/en/activities/tracking-SARS-CoV-2-variants.
(41) CDC | SARS-CoV-2 variant classifications and definitions. 2021, https://www.cdc.gov/coronavirus/2019-ncov/variants/variant-info.html (accessed 2021-12-31).
(42) Park, K. S.; Bazzill, J. D.; Son, S.; Nam, J.; Shin, S. W.; Ochyl, L. J.; Stuckey, J. A.; Meagher, J. L.; Chang, L.; Song, J.; Montefiori, D. C.; LaBranche, C. C.; Smith, J. L.; Xu, J.; Moon, J. J. Lipid-based vaccine nanoparticles for induction of humoral immune responses against HIV-1 and SARS-CoV-2. *J. Controlled Release* **2021**, *330*, 529−539.
(43) Huang, W. C.; Zhou, S.; He, X.; Chiem, K.; Mabrouk, M. T.; Nissly, R. H.; Bird, I. M.; Strauss, M.; Sambhara, S.; Ortega, J.; Wohlfert, E. A.; Martinez-Sobrido, L.; Kuchipudi, S. V.; Davidson, B. A.; Lovell, J. F. SARS-CoV-2 RBD neutralizing antibody induction is enhanced by particulate vaccination. *Adv. Mater.* **2020**, *32* (50), 2005637.
(44) WHO *COVID-19 vaccine tracker and landscape*, 2021. https://www.who.int/publications/m/item/draft-landscape-of-covid-19-candidate-vaccines (accessed 2021-12-31).
(45) Pallesen, J.; Wang, N.; Corbett, K. S.; Wrapp, D.; Kirchdoerfer, R. N.; Turner, H. L.; Cottrell, C. A.; Becker, M. M.; Wang, L.; Shi, W.; Kong, W. P.; Andres, E. L.; Kettenbach, A. N.; Denison, M. R.; Chappell, J. D.; Graham, B. S.; Ward, A. B.; McLellan, J. S. Immunogenicity and structures of a rationally designed prefusion MERS-CoV spike antigen. *Proc. Natl. Acad. Sci. U.S.A.* **2017**, *114* (35), 7348−7357.
(46) Crank, M. C.; Ruckwardt, T. J.; Chen, M.; Morabito, K. M.; Phung, E.; Costner, P. J.; Holman, L. A.; Hickman, S. P.; Berkowitz, N. M.; Gordon, I. J.; Yamshchikov, G. V.; Gaudinski, M. R.; Kumar, A.; Chang, L. A.; Moin, S. M.; Hill, J. P.; DiPiazza, A. T.; Schwartz, R. M.; Kueltzo, L.; Cooper, J. W.; Chen, P. F.; Stein, J. A.; Carlton, K.; Gall, J. G.; Nason, M. C.; Kwong, P. D.; Chen, G. L.; Mascola, J. R.; McLellan, J. S.; Ledgerwood, J. E.; Graham, B. S.; et al. A proof of concept for structure-based vaccine design targeting RSV in humans. *Science* **2019**, *365*, 505−509.
(47) Lu, M.; Dravid, P.; Zhang, Y.; Trivedi, S.; Li, A.; Harder, O.; Kc, M.; Chaiwatpongsakorn, S.; Zani, A.; Kenney, A.; Zeng, C.; Cai, C.; Ye, C.; Liang, X.; Shimamura, M.; Liu, S. L.; Mejias, A.; Ramilo, O.; Boyaka, P. N.; Qiu, J.; Martinez-Sobrido, L.; Yount, J. S.; Peeples, M. E.; Kapoor, A.; Niewiesk, S.; Li, J. A safe and highly efficacious measles virus-based vaccine expressing SARS-CoV-2 stabilized prefusion spike. *Proc. Natl. Acad. Sci. U.S.A.* **2021**, *118* (12), e2026153118.
(48) Cai, Y. F.; Zhang, J.; Xiao, T. S.; Peng, H. Q.; Sterling, S. M.; Walsh, R. M., Jr.; Rawson, S.; Rits-Volloch, S.; Chen, B. Distinct conformational states of SARS-CoV-2 spike protein. *Science* **2020**, *369*, 1586−1592.
(49) Liu, Z.; Xu, W.; Xia, S.; Gu, C.; Wang, X.; Wang, Q.; Zhou, J.; Wu, Y.; Cai, X.; Qu, D.; Ying, T.; Xie, Y.; Lu, L.; Yuan, Z.; Jiang, S. RBD-Fc-based COVID-19 vaccine candidate induces highly potent SARS-CoV-2 neutralizing antibody response. *Signal Transduct. Target. Ther.* **2020**, *5* (1), 282.
(50) Zhang, L.; Cao, L.; Gao, X. S.; Zheng, B. Y.; Deng, Y. Q.; Li, J. X.; Feng, R.; Bian, Q.; Guo, X. L.; Wang, N.; Qiu, H. Y.; Wang, L.; Cui, Z.; Ye, Q.; Chen, G.; Lu, K. K.; Chen, Y.; Chen, Y. T.; Pan, H. X.; Yu, J.; Yao, W.; Zhu, B. L.; Chen, J.; Liu, Y.; Qin, C. F.; Wang, X.; Zhu, F. C. A proof of concept for neutralizing antibody-guided vaccine design against SARS-CoV-2. *Natl. Sci. Rev.* **2021**, *8* (8), nwab053.
(51) Liu, C.; Ginn, H. M.; Dejnirattisai, W.; Supasa, P.; Wang, B.; Tuekprakhon, A.; Nutalai, R.; Zhou, D.; Mentzer, A. J.; Zhao, Y.; Duyvesteyn, H. M. E.; Lopez-Camacho, C.; Slon-Campos, J.; Walter, T. S.; Skelly, D.; Johnson, S. A.; Ritter, T. G.; Mason, C.; Clemens, S. A. C.; Naveca, F. G.; Nascimento, V.; Nascimento, F.; Costa, C. F. D.; Resende, P. C.; Pauvolid-Correa, A.; Siqueira, M. M.; Dold, C.; Temperton, N.; Dong, T.; et al. Reduced neutralization of SARS-CoV-2 B.1.617 by vaccine and convalescent serum. *Cell* **2021**, *184* (16), 4220−4236.
(52) Lucas, C.; Vogels, C. B. F.; Yildirim, I.; Rothman, J. E.; Lu, P.; Monteiro, V.; Gelhausen, J. R.; Campbell, M.; Silva, J.; Tabachikova, A.; Pena-Hernandez, M. A.; Muenker, M. C.; Breban, M. I.; Fauver, J. R.; Mohanty, S.; Huang, J.; et al. Impact of circulating SARS-CoV-2 variants on mRNA vaccine-induced immunity. *Nature* **2021**, *600*, 523−529.
(53) Cameroni, E.; Bowen, J. E.; Rosen, L. E.; Saliba, C.; Zepeda, S. K.; Culap, K.; Pinto, D.; VanBlargan, L. A.; De Marco, A.; di Iulio, J.; Zatta, F.; Kaiser, H.; Noack, J.; Farhat, N.; Czudnochowski, N.; Havenar-Daughton, C.; Sprouse, K. R.; Dillen, J. R.; Powell, A. E.; Chen, A.; Maher, C.; Yin, L.; Sun, D.; Soriaga, L.; Bassi, J.; Silacci-Fregni, C.; Gustafsson, C.; Franko, N. M.; Logue, J.; Iqbal, N. T.; Mazzitelli, I.; Geffner, J.; Grifantini, R.; Chu, H.; Gori, A.; Riva, A.; Giannini, O.; Ceschi, A.; Ferrari, P.; Cippà, P. E.; Franzetti-Pellanda, A.; Garzoni, C.; Halfmann, P. J.; Kawaoka, Y.; Hebner, C.; Purcell, L. A.; Piccoli, L.; Pizzuto, M. S.; Walls, A. C.; Diamond, M. S.; Telenti, A.; Virgin, H. W.; Lanzavecchia, A.; Snell, G.; Veesler, D.; Corti, D. Broadly neutralizing

https://doi.org/10.1021/acs.jmedchem.1c02025
J. Med. Chem. XXXX, XXX, XXX−XXX

antibodies overcome SARS-CoV-2 Omicron antigenic shift. *Nature* **2021**, DOI: 10.1038/s41586-021-04386-2.
(54) Zhang, L.; Li, Q.; Liang, Z.; Li, T.; Liu, S.; Cui, Q.; Nie, J.; Wu, Q.; Qu, X.; Huang, W.; Wang, Y. C. The significant immune escape of pseudotyped SARS-CoV-2 variant Omicron. *Emerg. Microbes. Infect.* **2022**, *11* (1), 1−5.
(55) Chen, X. Z.; Zhang, R. Y.; Wang, X. F.; Yin, X. G.; Wang, J.; Wang, Y. C.; Liu, X.; Du, J. J.; Liu, Z.; Guo, J. Peptide-free synthetic nicotine vaccine candidates with α-galactosylceramide as adjuvant. *Mol. Pharmaceutics* **2019**, *16* (4), 1467−1476.

https://doi.org/10.1021/acs.jmedchem.1c02025
J. Med. Chem. XXXX, XXX, XXX−XXX